


## Spin entanglement via scanning tunneling microscope current

Baruch Horovitz 

*Department of Physics, Ben Gurion University, Beer Sheva 84105, Israel*

Carsten Henkel 

*Institute of Physics and Astronomy, University of Potsdam, 14476 Potsdam, Germany*

 (Received 21 February 2021; revised 10 July 2021; accepted 30 July 2021; published 19 August 2021)

We consider a system of two spins under a scanning tunneling microscope bias and derive its master equation. We find that the tunneling elements to the electronic contacts (tip and substrate) generate an exchange interaction between the spins as well as a Dzyaloshinskii-Moriya interaction in the presence of spin-orbit coupling. The tunnel current spectrum then shows additional lines compared to conventional spin-resonance experiments. When the spins have degenerate Larmor frequencies and equal tunneling amplitudes (without spin orbit), there is a dark state with a vanishing decay rate. The coupling to the electronic environment generates significant spin-spin entanglement via the dark state, even if the initial state is nonentangled.

DOI: [10.1103/PhysRevB.104.L081405](https://doi.org/10.1103/PhysRevB.104.L081405)

Intense efforts are currently devoted to the study of two qubits coupled to an environment, motivated by quantum information science. In particular, it has been realized that dissipative dynamics due to qubits coupling to the same bath can be tuned to yield entangled states both in theory [1–4] and in experiment [5,6]. In parallel, there has been considerable effort in developing techniques of scanning tunneling microscopy (STM) to probe electron spin-resonance (ESR) features. These ESR-STM studies are of two types: either monitoring the current power spectrum in a DC bias employing a nonmagnetic tip [7–9] (first type) or monitoring the DC current with a magnetic tip when an additional AC voltage is tuned to resonance conditions [10–12].

In the present Letter we show that the STM setting with its two contacts provides another scenario for entangling two spins, representing two qubits (see sketch in Fig. 1). The presence of two nondegenerate spins has been proposed to account for the first type of ESR-STM phenomena [13]. Here we study the case of degenerate spins, which requires a different derivation of the appropriate master equation due to additional resonances. We find a number of phenomena: (i) The tunneling couplings to the electronic baths (tip and substrate) generate dissipation, but also an exchange coupling between the two spins; in the presence of spin-orbit coupling a Dzyaloshinskii-Moriya (DM) interaction also emerges. (ii) The spin-correlation functions as measured by an STM, in the presence of either exchange or dipole-dipole interactions, show additional spectral lines relative to those in conventional ESR. (iii) When the tunneling amplitudes of the two spins are equal, we identify a dark state, i.e., an entangled state with an infinite lifetime. An initial nonentangled state evolves into a significantly entangled state, i.e., environment-induced entanglement. In contrast to previously studied photon-induced entanglement [1–6], in our scenario the entanglement is electron induced and emerges in solid-state nanoscopic qubits, a

setup that is scalable and yet has a controllable low dephasing rate. Hence, it is a promising and realistic setup for quantum information devices.

In the following we use a system + bath formalism where a system-environment interaction sums products of operators  $A_j$ ,  $B_j$  in the system and environment spaces [14,15]. We choose the  $A_j$ 's such that they evolve in the interaction picture with frequency  $\nu_j$ ,

$$\mathcal{H}_{SE}(t) = \sum_j A_j e^{-i\nu_j t} B_j(t), \quad (1)$$

where the sum may contain one or more terms with  $\nu_j = 0$ . The master equation for the system density-matrix  $\rho$  is within the Born-Markov approximation,

$$\begin{aligned} \frac{d}{dt} \rho(t) &= \sum_{j,k} \{ \tilde{\Gamma}_{jk}(\nu_k) e^{-i(\nu_j + \nu_k)t} \\ &\quad \times [A_k \rho(t) A_j - A_j A_k \rho(t)] + \text{H.c.} \} \\ \tilde{\Gamma}_{jk}(\omega) &= \int_0^\infty d\tau \langle B_j(\tau) B_k(0) \rangle_E e^{i\omega\tau}, \end{aligned} \quad (2)$$

where  $\langle \dots \rangle_E$  denotes the bath average. In the following we apply the secular approximation, i.e., only terms  $j, k$  for which  $\nu_j + \nu_k = 0$  are kept, Eq. (2) then has the Lindblad form [14–16]. This is justified when finite frequency differences are much larger than the linewidth. It is important to note that we do include off-diagonal terms in view of degeneracies in our system.

We proceed to two isolated spins (quantum dots or impurities) described by Pauli matrices  $\tau \otimes \mathbb{1}$  and  $\mathbb{1} \otimes \tau$  (direct products display operators acting on the first spin times those acting on the second spin) and a common Larmor frequency  $\nu$  coupled by tunneling in parallel to the two environments  $L, R$  (Fig. 1). The latter have spin-independent energies  $\epsilon_{kL}, \epsilon_{kR}$

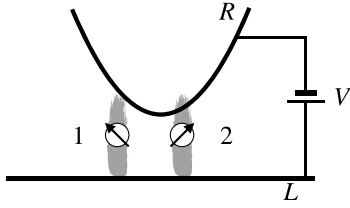


FIG. 1. Sketch of the system. The scanning tip and substrate are two electrodes  $R$  and  $L$  at a relative voltage  $V$ , they provide the environment for the spins labeled 1 and 2. A magnetic field yields a common Larmor frequency  $\nu$ . The environment-spin coupling is due to the tunneling, via the spin sites, between the electrodes. This allows, in particular, for spin flips via an effective exchange interaction between the tunneling electrons and the localized spins [Eq. (3)].

whose chemical potentials differ by a bias  $V$  and Hamiltonian  $\mathcal{H}_L = \sum_k \epsilon_{kL} c_{kL}^\dagger c_{kL}$  with electron creation and annihilation operators  $c_{kL}^\dagger, c_{kL}$ , being two-component spinors for each mode  $kL$ ; similarly with  $L \rightarrow R$ . Setting  $\mathcal{H}_0 = \frac{1}{2} \nu \tau_z \otimes \mathbb{1} + \frac{1}{2} \nu \mathbb{1} \otimes \tau_z$  ( $\hbar = 1$ ), the Hamiltonian is taken in the form

$$\begin{aligned} \mathcal{H} = & \mathcal{H}_0 + \mathcal{H}_L + \mathcal{H}_R + (J_1 c_R^\dagger \sigma_{c_L} \cdot \boldsymbol{\tau} \otimes \mathbb{1} \\ & + J_2 c_R^\dagger \sigma \hat{u} c_L \cdot \mathbb{1} \otimes \boldsymbol{\tau} + \text{H.c.}) \end{aligned} \quad (3)$$

where  $c_L = \sum_k c_{kL}$  is the local operator that couples to the spins (the same with  $L \rightarrow R$ ). The hopping terms  $J_{1,2}$  in Eq. (3) are derived from tunneling via a localized state that has strong on-site Coulomb repulsion, which eliminates doubly occupied or zero occupied electron states, a procedure known as the Schrieffer-Wolff transformation [13,17]. For spin 2, we use the unitary matrix  $\hat{u} = e^{i\sigma_z \phi} e^{i\sigma_y \theta/2}$  to model spin-orbit interactions; this is important for the coupling of an STM current to the spins [13]. There are additional terms that tunnel electrons from one lead and back to the same lead, however, the terms in (3) dominate at large voltage, i.e.,  $V \gg \nu, k_B T$  ( $T$  is the temperature), the typical case in STM experiments.

The interaction picture relative to  $\mathcal{H}_0 + \mathcal{H}_L + \mathcal{H}_R$  leads to  $\mathcal{H}_{SE}(t)$  in the form (1) with [using  $\tau_\pm = \frac{1}{2}(\tau_x \pm i\tau_y)$ ,  $\epsilon_{RL} = \epsilon_R - \epsilon_L$ , and an implicit summation over the bath levels  $k$ ],

$$\begin{aligned} A_1 &= \tau_- \otimes \mathbb{1}, \quad \nu_1 = \nu, \\ B_1 &= 2J_1 (c_R^\dagger \sigma_+ c_L e^{i\epsilon_{RL}t} + c_L^\dagger \sigma_+ c_R e^{-i\epsilon_{RL}t}) \\ A_z &= \tau_z \otimes \mathbb{1}, \quad \nu_z = 0, \\ B_z &= J_1 c_R^\dagger \sigma_z c_L e^{i\epsilon_{RL}t} + \text{H.c.} \\ A_2 &= \mathbb{1} \otimes \tau_-, \quad \nu_2 = \nu, \\ B_2 &= 2J_2 (c_R^\dagger \sigma_+ \hat{u} c_L e^{i\epsilon_{RL}t} + c_L^\dagger \hat{u}^\dagger \sigma_+ c_R e^{-i\epsilon_{RL}t}), \\ A_{z'} &= \mathbb{1} \otimes \tau_z, \quad \nu_{z'} = 0, \\ B_{z'} &= J_2 c_R^\dagger \sigma_z \hat{u} c_L e^{i\epsilon_{RL}t} + \text{H.c.} \end{aligned} \quad (4)$$

(Two additional terms are  $A_{-j} = A_j^\dagger$  with  $\nu_{-1,-2} = -\nu$ .) The product  $A_z A_{z'}$  is secular and produces off-diagonal terms as well as  $A_1 A_{-2} = A_1 A_2^\dagger$  or  $A_{-1} A_2 = A_1^\dagger A_2$ . Plugging these expressions into Eq. (2) is straightforward and is detailed in the

Supplemental Material (SM) [18]. Here we outline the form of one particular term,

$$\begin{aligned} \frac{d\rho}{dt} = & \dots + \tilde{\Gamma}_{2,-1}(-\nu) [A_{-1} \rho A_2 - A_2 A_{-1} \rho] + \text{H.c.} \\ \tilde{\Gamma}_{2,-1}(-\nu) = & 4J_1 J_2 N^2(\epsilon_F) \cos \frac{1}{2} \theta e^{-i\phi} \\ & \times \int_{\epsilon_L, \epsilon_R} i \left\{ \frac{f_R(1-f_L)}{\epsilon_{RL} - \nu + i0} - \frac{f_L(1-f_R)}{\epsilon_{RL} + \nu - i0} \right\} \end{aligned} \quad (5)$$

where  $\text{Tr}[\sigma_+ \hat{u} \sigma_-] = \text{Tr}[\hat{u}^\dagger \sigma_+ \sigma_-] = \cos \frac{1}{2} \theta e^{-i\phi}$  is used,  $f_R = f_R(\epsilon_R)$ ,  $f_L = f_L(\epsilon_L)$  are the Fermi distributions, containing the bias  $V$ , and  $N^2(\epsilon_F)$  is the product of the two electronic densities of states at the Fermi energy. We note that the principal value (P) of this integral is strongly cutoff dependent, the cutoff  $\Lambda$  being the electronic bandwidth on either tip or substrate, assumed comparable; the  $\nu$  dependence in this term is weak provided  $\nu \ll \Lambda$ . The result is then for  $e^{-(V \pm \nu)/k_B T} \ll 1$ ,

$$\begin{aligned} \tilde{\Gamma}_{2,-1}(-\nu) = & 4J_1 J_2 N^2(\epsilon_F) \cos \frac{1}{2} \theta e^{-i\phi} \\ & \times [\pi(V - \nu) - i\Delta + i\nu \ln(V/\Lambda)] \\ \Delta = & \text{P} \int_{\epsilon_R, \epsilon_L} \frac{f_L - f_R}{\epsilon_R - \epsilon_L} \\ \approx & \Lambda \ln \frac{16\Lambda^2}{|\Lambda^2 - V^2|} - V \ln \left| \frac{\Lambda + V}{\Lambda - V} \right|. \end{aligned} \quad (6)$$

This assumes constant densities of states so that the expression for  $\Delta$  is taken just as an approximate indication that this term increases linearly with  $\Lambda$  and, therefore, can be large. Collecting all the secular terms that couple the two spins, i.e.,  $\tilde{\Gamma}_{jk}(\nu_k)$  with  $(j, k) = (2, -1), (-2, 1), (1, -2), (-1, 2), (z, z'), (z', z)$  as given in the SM [18], their imaginary parts combine into the effective interaction Hamiltonian,

$$\begin{aligned} \mathcal{H}_{\text{int}} = & -J_{\text{ex}} \boldsymbol{\tau}_1 \cdot \boldsymbol{\tau}_2 + J_{\text{DM}} [\boldsymbol{\tau}_1 \times \boldsymbol{\tau}_2]_z, \\ \left. \begin{aligned} J_{\text{ex}} \\ J_{\text{DM}} \end{aligned} \right\} = & 4J_1 J_2 N^2(\epsilon_F) \Delta \cos \frac{1}{2} \theta \begin{cases} \cos \phi, \\ \sin \phi. \end{cases} \end{aligned} \quad (7)$$

We recognize an exchange coupling as well as a Dzyaloshinskii-Moriya interaction. The latter appears in the presence of spin-orbit coupling ( $\phi \neq 0$ ) which breaks the symmetry between the two spins. We note that these bath-induced interactions are similar in spirit to the well-known Ruderman-Kittel-Kasuya-Yosida (RKKY) interaction that generates an exchange coupling between two distant spins in a metal, the metal being a common reservoir [19]. Recall that the RKKY coupling is also sensitive to the cutoff as well as to the dimensionality of the metal.

The environment-induced interaction can be detected in correlation functions that are measured by either an ESR or an STM probe. Consider the correlations,

$$\begin{aligned} C_1(\omega) = & \langle (\tau_- \otimes \tau_z + \tau_z \otimes \tau_-)_t (\tau_+ \otimes \tau_z + \tau_z \otimes \tau_+)_0 \rangle_\omega \\ & + (\omega \rightarrow -\omega), \\ C_2(\omega) = & \langle (\tau_- \otimes \tau_z)_t (\tau_+ \otimes \tau_z)_0 \rangle_\omega + (\omega \rightarrow -\omega), \\ C_3(\omega) = & \langle (\tau_- \otimes \tau_+)_t (\tau_+ \otimes \tau_-)_0 \rangle_\omega + (\omega \rightarrow -\omega). \end{aligned} \quad (8)$$

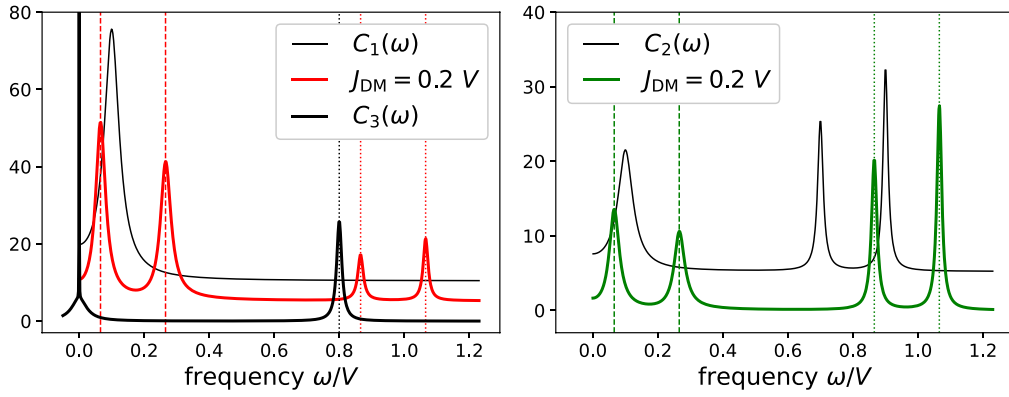


FIG. 2. Correlations  $C_1(\omega)$ ,  $C_3(\omega)$  (left) and  $C_2(\omega)$  (right) of Eq. (8) with the parameters: Larmor frequency  $\nu = 0.1$  V (including the bath-induced shift), electrode couplings  $\lambda_1 = 0.01$ ,  $\lambda_2 = 0.009$  where  $\lambda_j = 16\pi J_j^2 N^2(\epsilon_F)$ , ( $j = 1, 2$ ), spin-orbit angle  $\theta = 0$  and exchange interaction  $J_{\text{ex}} = 0.2$  V. Black lines:  $\phi = 0$ , no DM interaction; the peaks are at the expected positions  $\omega = \nu$  for  $C_1(\omega)$ ,  $\omega = \nu, 4J_{\text{ex}} \pm \nu$  for  $C_2(\omega)$ , and  $\omega = 0, 4J_{\text{ex}}$  for  $C_3(\omega)$ . Thick colored lines: allowing for both exchange  $J_{\text{ex}} = 0.2$  V and DM interaction  $J_{\text{DM}} = 0.2$  V (i.e.,  $\phi = \pi/4$ ). The vertical dashed and dotted lines mark the transitions expected from the energy spectrum (9).  $C_3(\omega)$  has a near  $\delta(\omega)$  peak as well as a finite-width peak at  $\omega = 0$  whose widths correspond to the inverse lifetimes of the dark and bright states, respectively. Spectra are shifted vertically for clarity.

Here  $C_1(\omega)$  probes both spins equally as in macroscopic ESR, whereas  $C_2(\omega)$  probes only one spin as allowed with STM. We recall that STM probes the spins via the current correlations [8], the current being  $iJ_1 c_R^\dagger \sigma c_L \cdot \tau \otimes \mathbb{1} + iJ_2 c_R^\dagger \sigma \hat{u} c_L \cdot \mathbb{1} \otimes \tau + \text{H.c.}$  The spin-dependent current fluctuations, therefore, involve either  $\tau_\pm$  for the spin flip or  $\tau_z$ , otherwise. The current fluctuations allow also for a double spin flip, hence, detection of the correlation  $C_3(\omega)$ . The correlation functions are computed from the quantum regression formula, see the SM [18]. To identify the various lines, we diagonalize the system Hamiltonian including  $\mathcal{H}_{\text{int}}$ ,

$$\begin{aligned} \frac{1}{\sqrt{2}}[|\uparrow\downarrow\rangle - e^{i\psi}|\downarrow\uparrow\rangle]: \quad E_S &= 2\sqrt{J_{\text{ex}}^2 + J_{\text{DM}}^2} + J_{\text{ex}} \\ |\uparrow\uparrow\rangle: \quad E_{T1} &= \nu - J_{\text{ex}}, \\ \frac{1}{\sqrt{2}}[|\uparrow\downarrow\rangle + e^{i\psi}|\downarrow\uparrow\rangle]: \quad E_{T2} &= -2\sqrt{J_{\text{ex}}^2 + J_{\text{DM}}^2} + J_{\text{ex}}, \\ |\downarrow\downarrow\rangle: \quad E_{T3} &= -\nu - J_{\text{ex}}, \end{aligned} \quad (9)$$

where  $\tan \psi = J_{\text{DM}}/J_{\text{ex}}$ . If both interactions are strictly within our model (7), then remarkably,  $\psi = \phi$ , the spin-orbit phase. We use the labels  $S$  and  $T$  for the singlet and the triplet, although these coincide with the exact eigenstates only for  $J_{\text{DM}} = 0$ .

Consider first the exchange-only case  $\phi = 0$ . An ESR experiment allows only transitions within the triplet states, and all appear at frequency  $\nu$ . There are no transitions between the singlet and the triplet states because of their opposite permutation symmetry, while the probing field is uniform in space. In contrast, a STM experiment allows the probing current to tunnel via only one spin, hence, permutation symmetry does not hold. The experiment would then show also singlet to triplet transitions, i.e., total of three lines at  $\nu, \nu + 4J_{\text{ex}}, |\nu - 4J_{\text{ex}}|$  as shown in Fig. 2(right). Thus, ESR-STM reveals the spectra of the two-spin system in more detail.

The case with spin-orbit coupling where both  $J_{\text{ex}}$  and  $J_{\text{DM}}$  are nonzero is asymmetric within the pair (only the coupling

to the second spin involves the spin-orbit matrix), hence, both ESR and STM yield four lines:  $\nu \pm 2(\sqrt{J_{\text{ex}}^2 + J_{\text{DM}}^2} - J_{\text{ex}})$  (the previous line at  $\nu$  is split), and  $2(\sqrt{J_{\text{ex}}^2 + J_{\text{DM}}^2} + J_{\text{ex}}) \pm \nu$ . This case is shown in Fig. 2(left):  $C_1(\omega)$  shows indeed four lines, although the additional two are rather weak. The STM case represented by  $C_2(\omega)$  has four lines of comparable intensity.

The spectrum of  $C_3$  shows a resonance at  $4J_{\text{ex}}$  at the symmetric point [Fig. 2(left)] because the operator  $(\tau_- \otimes \tau_+) \rho_{\text{st}}$  contains a superposition of  $S$  and  $T2$  states with different energies. A projection onto the entangled subspace may be achieved by detecting this resonance since  $\tau_- \otimes \tau_+$  maps the nonentangled states  $|\uparrow\uparrow\rangle$  and  $|\downarrow\downarrow\rangle$  to zero.

We exhibit now the entanglement between the spins, induced by their interaction with the electronic bath, similar to works on two-qubit systems coupled by either a plasmonic waveguide [3] or by the cavity electrodynamics [4]. The most promising situation emerges when the spins are equally coupled to the environments  $J_1 = J_2$  and  $\theta = \phi = 0$  so that the spin orbit interaction does not distinguish between the spins. We then observe that the singlet state  $|d\rangle = [|\uparrow\downarrow\rangle - |\downarrow\uparrow\rangle]/\sqrt{2}$  becomes dark, meaning that it decouples from the three triplet states. For the dark-state projector,

$$\begin{aligned} \hat{d} &= \frac{1}{2}(|\uparrow\downarrow\rangle - |\downarrow\uparrow\rangle)(\langle\uparrow\downarrow| - \langle\downarrow\uparrow|) \\ &= \frac{1}{4}\mathbb{1} \otimes \mathbb{1} - \frac{1}{4}\tau_z \otimes \tau_z - \frac{1}{2}\tau_- \otimes \tau_+ - \frac{1}{2}\tau_+ \otimes \tau_-, \end{aligned} \quad (10)$$

we can show from the master equation that  $dp_d/dt = \text{Tr}[\hat{d}(d\rho/dt)] = 0$  (see the SM [18]), i.e., its decay rates vanish precisely. The stationary state turns out to be a one-parameter family that interpolates between  $\hat{d}$  and a mixture  $\rho_{\text{tr}}$  of triplet states with quasithermal populations (its effective temperature is  $\approx \frac{1}{2}V/k_B$  provided  $V \gg \nu$ ). This remarkable phenomenon of a range of steady states is exhibited by

$$\begin{aligned} \langle\tau_z \otimes \mathbb{1}\rangle &= \langle\mathbb{1} \otimes \tau_z\rangle = -\tilde{\nu}(1 + 2\rho_{+-}), \\ \langle\tau_z \otimes \tau_z\rangle &= \tilde{\nu}^2 + 2(1 + \tilde{\nu}^2)\rho_{+-}, \end{aligned} \quad (11)$$

where  $\tilde{\nu} = \nu/V$  and  $\rho_{+-} = \langle\tau_+ \otimes \tau_-\rangle$  is an arbitrary real parameter, constrained only by the eigenvalues of  $\rho$  being

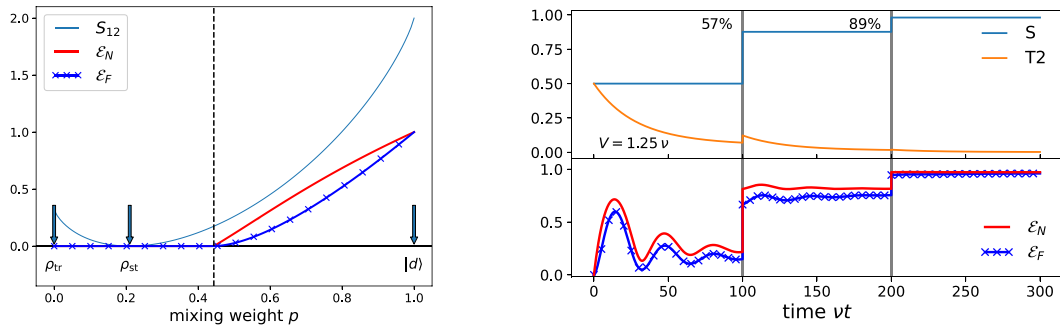


FIG. 3. (Left) Entanglement measures at the symmetric point  $\lambda_1 = \lambda_2$ ,  $\theta = \phi = 0$ : the steady state is given by a one-parameter family that interpolates between a mixed state  $\rho_{tr}$  in the triplet subspace (left, weight  $1 - p$ ) and the dark state (right, weight  $p$ ). The third arrow marks the noncorrelated stationary state  $\rho_{st}$  that is also found when the parameters are slightly detuning from the symmetric point. Thin blue line: quantum mutual information  $S_{12}$ , nonzero nearly everywhere, but not specific to entanglement. Thick red lines: logarithmic negativity  $\mathcal{E}_N$ , thick blue lines with symbols: entanglement of formation  $\mathcal{E}_F$ , dashed vertical line: critical mixing parameter  $p_c$  (see the main text). Mutual information and entanglement measures are scaled to (e)bits, using logarithms to base 2; we take  $V = 2.5\nu$ . (Right) Transient entanglement at the symmetric point, followed by probabilistic “purification.” Starting from the product state  $|\uparrow\downarrow\rangle$ , the entanglement of the two-qubit system transiently oscillates since the states  $|\uparrow\downarrow\rangle$  and  $|\downarrow\uparrow\rangle$  are mixed by a Rabi frequency of  $2J_{ex}$ . The singlet state population ( $S$ ) remains constant, whereas the triplet sector relaxes to thermal equilibrium (only the  $S$  and  $T2$  populations are shown; details about the transient entanglement, such as oscillations and decoherence are discussed in the SM [18]). The vertical lines mark measurements of the  $\tau_z \otimes \tau_z$  spin correlation, and provided the result is  $-1$  (the percentage given in the top panel), they increase the entanglement because the system is projected into the subspace spanned by the states  $S$ ,  $T2$ . Thus, both environment-induced relaxation as well as the measurement protocol contribute to the enhancement of entanglement. The time evolution is computed from the eigenvalue spectrum of the master equation (see the SM [18]). Parameters:  $\lambda = 0.0126$ ,  $J_{ex} \approx 0.024\nu$ , voltage  $V = 1.25\nu$  so that  $p_c = 0.229$ .

less than 1. The parameter  $\rho_{+-}$  can also be detected from the  $\delta(\omega)$  peak in the correlation spectrum  $C_3(\omega)$  [Eq. (8), in Fig. 2(left) the near-degenerate case is shown]. Figure 3(left) quantifies the entanglement in this family of stationary states as measured by the entanglement of formation  $\mathcal{E}_F$  (related to the concurrence [20]) and the logarithmic negativity [21,22]  $\mathcal{E}_N$ . When the weight  $p$  of the dark state exceeds  $p_c = \frac{1}{2}(1 - \tilde{\nu}^2)/(1 - \tilde{\nu}^2/3)$  (dashed line), there is stationary entanglement. When lowering  $V$  towards  $\nu$  (but keeping  $e^{-(V-\nu)/k_B T} \ll 1$ ),  $p_c$  is decreased: a larger range of equilibrium states is then entangled.

In Fig. 3(right), we show that an initially nonentangled state  $|\uparrow\downarrow\rangle$  builds up entanglement during the relaxation of the triplet sector to equilibrium. The weight of the dark state does not exceed  $p = \frac{1}{2}$  with this easy-to-prepare product state, and this is why we propose in Fig. 3(right) a route of further increasing the entanglement. At the vertical gray lines, a measurement of the spin-spin correlation  $\tau_z \otimes \tau_z$  is made: From the result  $-1$ , the experimenter may infer that the two spins are not in the product states  $|\uparrow\uparrow\rangle$  or  $|\downarrow\downarrow\rangle$ , without destroying the relative phase of any entangled state. A successful result, thus, increases the relative weight of the dark state. As the system relaxes, the  $T2$  state is depleted, and the entanglement increases slightly. The measurement can be repeated and, if successful, purifies the dark state further. To actually perform

such a measurement, one may monitor the peaks at  $\omega = 0$  or at  $\omega = 4J_{ex}$  of the current fluctuation spectrum  $C_3(\omega)$ . These peaks signal the double spin-flip process, hence, once observed the system collapses into the  $S$  or  $T2$  states, equivalent to detecting an eigenvalue  $-1$  of  $\tau_z \otimes \tau_z$ . We note that this procedure does not detect every double spin flip since it should be made fast compared with the lifetime of the bright state so as to avoid generating the product states  $T1$ ,  $T3$ . A more detailed analysis is left for future work.

In conclusion, we have shown a number of resonance phenomena that can be achieved by probing a pair of degenerate impurity spins in the tunneling junction of a STM. These phenomena include generating exchange and DM interactions between the spins, the observation of additional lines in the STM setup, providing more information on the two-spin state. In some cases, a maximally entangled dark state emerges that is highly significant for quantum information applications.

This work has been supported by the Deutsche Forschungsgemeinschaft through the German-Israeli partnership Program DIP (Project “Quantum Phenomena in Hybrid Systems,” Grant Nos. Schm-1049/7-1 and Fo 703/2-1). B.H. thanks G. Zaránd for stimulating and useful discussions and Y. Manassen for insights on relevant experimental features.

- [1] A. F. Alharbi and Z. Ficek, Deterministic creation of stationary entangled states by dissipation, *Phys. Rev. A* **82**, 054103 (2010).  
 [2] M. J. Kastoryano, F. Reiter, and A. S. Sorensen, Dissipative Preparation of Entanglement in Optical Cavities, *Phys. Rev. Lett.* **106**, 090502 (2011).

- [3] D. Martín-Cano, A. González-Tudela, L. Martín-Moreno, F. J. García-Vidal, C. Tejedor, and E. Moreno, Dissipation-driven generation of two-qubit entanglement mediated by plasmonic waveguides, *Phys. Rev. B* **84**, 235306 (2011).

- [4] Z. Ficek and R. Tanas, Entangled states and collective non-classical effects in two-atom systems, *Phys. Rep.* **372**, 369 (2002).
- [5] J. T. Barreiro *et al.*, An open-system quantum simulator with trapped ions, *Nature (London)* **470**, 486 (2011).
- [6] H. Krauter, C. A. Muschik, K. Jensen, W. Wasilewski, J. M. Petersen, J. I. Cirac, and E. S. Polzik, Entanglement Generated by Dissipation and Steady State Entanglement of Two Macroscopic Objects, *Phys. Rev. Lett.* **107**, 080503 (2011).
- [7] Y. Manassen, R. J. Hamers, J. E. Demuth, and J. A. J. Castellano, Direct Observation of the Precession of Individual Paramagnetic Spins on Oxidized Silicon Surfaces, *Phys. Rev. Lett.* **62**, 2531 (1989).
- [8] A. V. Balatsky, M. Nishijima, and Y. Manassen, Electron spin resonance-scanning tunneling microscopy, *Adv. Phys.* **61**, 117 (2012).
- [9] Y. Manassen, M. Averbukh, M. Jbara, B. Siebenhofer, A. Shnirman, and B. Horovitz, Fingerprints of single nuclear spin energy levels using STM-ENDOR, *J. Mag. Res.* **289**, 107 (2018).
- [10] S. Müllegger, S. Tebi, A. K. Das, W. Schöfberger, F. Faschinger, and R. Koch, Radio Frequency Scanning Tunneling Spectroscopy for Single-Molecule Spin Resonance, *Phys. Rev. Lett.* **113**, 133001 (2014).
- [11] S. Baumann, W. Paul, T. Choi, C. P. Lutz, A. Ardavan, and A. J. Heinrich, Electron paramagnetic resonance of individual atoms on a surface, *Science* **350**, 417 (2015).
- [12] P. Willke *et al.*, Probing quantum coherence in single-atom electron spin resonance, *Sci. Adv.* **4**, eaaq1543 (2018).
- [13] B. Horovitz and A. Golub, Double quantum dot scenario for spin resonance in current noise, *Phys. Rev. B* **99**, 241407(R) (2019).
- [14] A. Shnirman and I. Kamleitner, Physics of Quantum Information, 2012, lecture notes, online at [www.tkm.kit.edu/downloads/QC-SCRIPT.pdf](http://www.tkm.kit.edu/downloads/QC-SCRIPT.pdf).
- [15] M. Schlosshauer, *Decoherence and the Quantum-to-Classical Transition* (Springer, Berlin/Heidelberg, 2007), Chap. 4.
- [16] F. Nathan and M. S. Rudner, Universal Lindblad equation for open quantum systems, *Phys. Rev. B* **102**, 115109 (2020).
- [17] A. C. Hewson, *The Kondo Problem to Heavy Fermions* (Cambridge University Press, Cambridge, UK, 1993).
- [18] See Supplemental Material at <http://link.aps.org/supplemental/10.1103/PhysRevB.104.L081405> for details on the derivation of the master equation, evaluation of spin entanglement, additional interactions, and spectra, which includes Refs. [23–37].
- [19] C. Kittel, in *Solid State Physics*, edited by F. Seitz, D. Turnbull, and H. Ehrenreich (Academic, New York, 1969), Vol. 22, Chap. 1, pp. 1–26.
- [20] W. K. Wootters, Entanglement of Formation of an Arbitrary State of Two Qubits, *Phys. Rev. Lett.* **80**, 2245 (1998).
- [21] A. Peres, Separability Criterion for Density Matrices, *Phys. Rev. Lett.* **77**, 1413 (1996).
- [22] M. Horodecki, P. Horodecki, and R. Horodecki, Separability of mixed states: Necessary and sufficient conditions, *Phys. Lett. A* **223**, 1 (1996).
- [23] F. Bloch, Generalized theory of relaxation, *Phys. Rev.* **105**, 1206 (1957).
- [24] A. G. Redfield, On the theory of relaxation processes, *IBM J. Res. Dev.* **1**, 19 (1957).
- [25] R. Alicki and K. Lendi, *Quantum Dynamical Semigroups and Applications*, Lecture Notes in Physics, Vol. 717 (Springer, Berlin/Heidelberg, 2007).
- [26] O. Parcolet and C. Hooley, Perturbative expansion of the magnetization in the out-of-equilibrium Kondo model, *Phys. Rev. B* **66**, 085315 (2002).
- [27] S. Miyahara, J.-B. Fouet, S. R. Manmana, R. M. Noack, H. Mayaffre, I. Sheikin, C. Berthier, and F. Mila, Uniform and staggered magnetizations induced by Dzyaloshinskii-Moriya interactions in isolated and coupled spin-1/2 dimers in a magnetic field, *Phys. Rev. B* **75**, 184402 (2007).
- [28] A. Beige, S. Bose, D. Braun, S. F. Huelga, P. L. Knight, M. B. Plenio, and V. Vedral, Entangling atoms and ions in dissipative environments, *J. Mod. Opt.* **47**, 2583 (2000).
- [29] Z. Ficek and R. Tanaš, Entanglement induced by spontaneous emission in spatially extended two-atom systems, *J. Mod. Opt.* **50**, 2765 (2003).
- [30] G. Shavit, B. Horovitz, and M. Goldstein, Bridging between laboratory and rotating-frame master equations for open quantum systems, *Phys. Rev. B* **100**, 195436 (2019), see e.g. Appendix B.
- [31] R. F. Werner, Quantum states with Einstein-Podolsky-Rosen correlations admitting a hidden-variable model, *Phys. Rev. A* **40**, 4277 (1989).
- [32] G. Vidal and R. F. Werner, Computable measure of entanglement, *Phys. Rev. A* **65**, 032314 (2002).
- [33] J. P. Paz and A. J. Roncaglia, Dynamics of the Entanglement between Two Oscillators in the Same Environment, *Phys. Rev. Lett.* **100**, 220401 (2008).
- [34] J. Onam González, L. A. Correa, G. Nocerino, J. P. Palao, D. Alonso, and G. Adesso, Testing the Validity of the ‘Local’ and ‘Global’ GKLS Master Equations on an Exactly Solvable Model, *Open Sys. Inf. Dyn.* **24**, 1740010 (2017).
- [35] J. E. Wertz and J. R. Bolton, *Electron Spin Resonance, Elementary Theory and Practical Applications* (McGraw-Hill, New York, 1986), Chap. 10.
- [36] I. Martin, A. Shnirman, L. Tian, and P. Zoller, Ground-state cooling of mechanical resonators, *Phys. Rev. B* **69**, 125339 (2004).
- [37] A. Abragam and B. Bleaney, *Electron Paramagnetic Resonance of Transition Ions, Oxford Classic Texts in the Physical Sciences* (Clarendon, Oxford, 2012).